Large Area Optimized Thin Film Nano Solar Cells on Metal Sheet

M. Toivola, T. Peltola, K. Miettunen, J. Halme, K. Aitola, P. D. Lund

Helsinki University of Technology, Department of Applied Physics, Advanced Energy Systems, P. O. Box 5100, FIN-02015 TKK, Finland

Tel.: +358 9 451 8254, Fax: +358 9 451 3195, Email: minna.toivola@tkk.fi

ABSTRACT

Nanostructured dye solar cell (DSC) "mini-module", size 6 cm x 6 cm with ~15 cm^2 active area directly integrated on a stainless steel (StS) sheet has been demonstrated. With a configuration where the StS works as the photoelectrode (PE) substrate and the counter electrode (CE) is prepared on conducting glass or ITO-PET plastic foil, 3.4 % and 2.5 % total power conversion efficiencies, respectively, have been gained. Compared to results obtained with small, 1.6 cm x 2 cm cells with 0.32 cm^2 active area prepared with the same methods and materials, i. e. 3.4 % efficiency with a StS PE and an ITO-PET CE, the large cell performance is not far behind. These efficiencies are also amongst the highest reported in the literature for this kind of a DSC configuration. Flexible structure enables high throughput roll to roll type industrial manufacturing of the cells and cost-efficient substrate materials make production of even modest efficiency cells economically feasible.

Keywords: dye solar cell, metal substrate, flexible, upscaling

1 INTRODUCTION

During the last few years, dye solar cell (DSC) [1] technology has emerged as a potential alternative and a follower to the more traditional solid semiconductor photovoltaic devices, due to cost-efficient materials and simple manufacturing methods of the DSC. Operating principle of the DSC, as presented in Figure 1, resembles the photosynthesis reaction of the green plants. Electrons are released in the photoactive dye molecules adsorbed on a porous, high active surface area network of TiO_2 nanoparticles (the photoelectrode, PE), through which they diffuse to the conducting substrate which works as the current collector, and are transferred to an external circuit. From there the electrons return to the counter electrode (CE) where they reduce the positive hole born in the dye photoexcitation process and transported to the CE by the redox couple of the electrolyte. In short, the cell operation is based on consecutive oxidation/reduction cycles – no chemical substances are consumed or permanently transformed in the process. The highest photon-to-energy conversion efficiencies are obtained with ruthenium-based organometallic dyes in conjunction with the iodide/triiodide redox couple.

At the moment, the DSC technology is already on the verge of commercialization [2] but one of the still remaining challenges is the rigid and fragile glass substrate typically used in the cells. We have investigated an alternative DSC structure, in which the PE is deposited on a stainless steel (StS) sheet and the CE on a plastic foil, as presented in Figure 2. This kind of a flexible cell structure enables high throughput industrial scale roll to roll manufacturing of the cells and provides economical savings, taken that the glass substrate is still one of the most expensive cell components. Metal substrate has also many additional benefits, such as superior electrical conductivity, tolerance to high temperatures which enables sintering of the PE film, smaller leakage (recombination) current than from other substrates [3], and mechanical robustness. Direct integration of the DSC structure on e. g. roofing and other building materials would also greatly facilitate implementation of this technology since no additional supporting stands for the panels would be needed.

This paper is a continuation to our previous studies on StS-based DSCs [3 – 4]. We report here results from tests on cell size upscaling from small, laboratory-type test cells to substantially larger area "mini-modules" and discuss the special requirements and challenges of the process, preparation technique and material-wise.
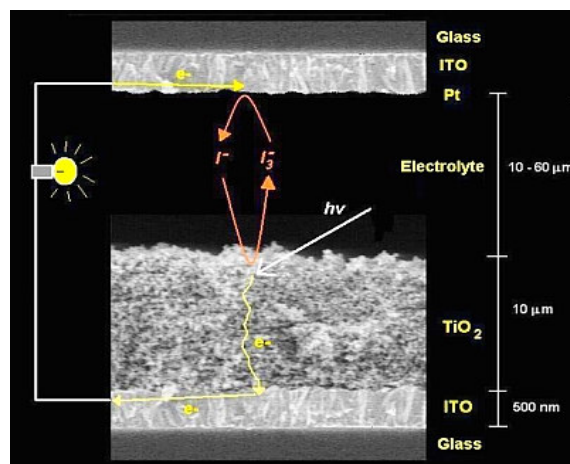
Figure 1: Cross-sectional scanning electron micrograph showing the operating principle of the DSC.
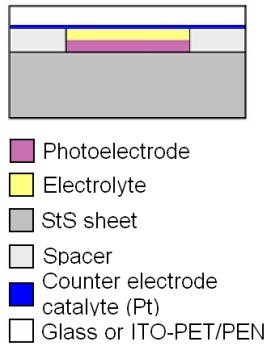
Figure 2: Schematic of the StS-based DSC.

2 EXPERIMENTAL

2.1 Cell Preparation

6 cm x 6 cm sized stainless steel sheets (type 1.4301, thickness 1 – 1.25 mm; supplied by Outokumpu) were used as the PE substrates whereas both ITO-PET (thickness 0.2 mm, sheet resistance 60 Ω/sq., Bekaert) and ITO-PEN (thickness 0.2 mm, sheet resistance 15 Ω/sq., Peccell) were employed as the CE substrates. As a reference, CEs were prepared also on FTO glass (TEC-15, thickness 2.5 mm, sheet resistance 15 Ω/sq., Pilkington). Details of the substrate pre-treatment and other steps of the cell preparation can be found from our previous publications [3 – 5]. In short, the PE films were deposited on the StS sheets with the doctor-blading method using commercial TiO_2 paste (Sustainable Technologies International). Two layers were spread, resulting in film thickness of 10 – 15 μm after which the films were sintered in 450 – 500 ^{o}C for 30 minutes. The plastic CE substrates were catalyzed by sputtering a 1 – 2 nm layer of platinum on them, whereas for the FTO glass, the standard thermal platinization method (resulting in similar Pt film thickness) [6] was used. The electrolyte composition was 0.5 M LiI, 0.05 M I_2, and 0.5 M 4-*tert*-butylpyridine (TBP) in 3-methoxypropionitrile. The electrodes were sealed together with thermoplastic Surlyn ionomer resin film after which the electrolyte was injected into the cells through holes drilled in the StS sheet.

2.2 Model for the Cell Geometry Optimization

The superior electrical conductivity of the StS enables substantial enlargening of the PE film size without ohmic losses but in the case of the CE substrate, especially ITO-PET with its relatively high sheet resistance, additional current collector structures are needed on the CE. To optimize their geometry, a semi-empirical model based on partial differential equations describing the current flow in the cell and a slightly "expanded" standard solar cell equivalent circuit (Figure 3.) was developed for this purpose [7]. The model takes into account the real cell dimensions and materials in the form of varying substrate surface conductivity, so all kinds of substrate material combinations (glass-glass, glass-StS, plastic-StS, etc.) can be modeled with it. A measured small DSC *IV*-curve is used as the source data and the model approximates the large cell as an "infinite" array of parallel current generators behaving like an infinitesimally small DSC. The model was solved with COMSOL Multiphysics finite element method solver (COMSOL, Inc.).
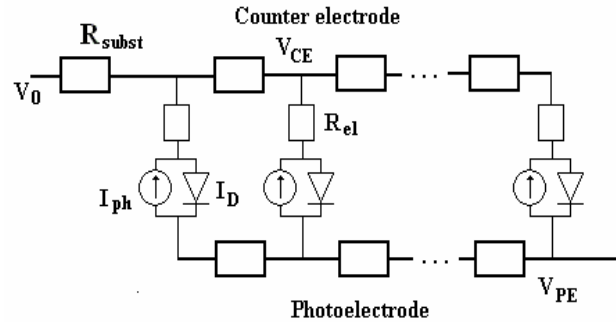
Figure 3: Equivalent circuit for the large DSC. The parallel connection of a photocurrent term (I_{ph}) and a diode (I_D; describing the recombination losses) models the current generation at the PE.

2.3 Measurements

The cells were characterized with current-voltage(*IV*)-curve measurements in a custom-built solar simulator with ten 150 W halogen lamps as the illumination source, a temperature-controlled measurement plate and a calibrated monocrystalline silicon reference cell with which the lamp intensity could be adjusted to the standard 100 mW/cm^2. The spectral mismatch factor of the simulator [8] was used to make the *IV*-curves correspond to the AM1.5G solar irradiation.

3 RESULTS AND DISCUSSION

3.1 Optimized CE Current Collector and TiO$_2$ Layer Geometry

The results of the modeling described in Chapter 2.2 are presented in Figure 4 and Table 1. In short, due to ohmic losses on the (CE) substrate surface current flow in a large cell is always uneven but with careful optimization of the current collector geometry a satisfactory trade-off between the ohmic and active area losses (i. e. TiO$_2$-free area under the current collectors) can be reached. Table 1 summarizes the cell efficiencies and efficiency losses with different substrate sheet and current collector stripe resistance combinations, calculated with the model.

The final large StS-PE DSC geometries and dimensions are presented in Figure 5. In the case of the FTO glass and

ITO-PEN, which have lower sheet resistance, smaller number of the CE current collector stripes were needed whereas for ITO-PET, also the additional "widenings" on top of the substrate were deposited to facilitate more efficient current flow to the main current collector (not shown in figure). Inkjet-printing of silver nanoparticle ink (Advanced Nano Products) was used as the deposition method for the additional CE current collector stripes. A satisfactory stripe resistivity of < 30 Ω/cm was obtained with two layers of ink (stripe width ca. 1 mm). Since the electrolyte corrodes silver, the stripes were protected against it by melting a strip of Surlyn on top of them.
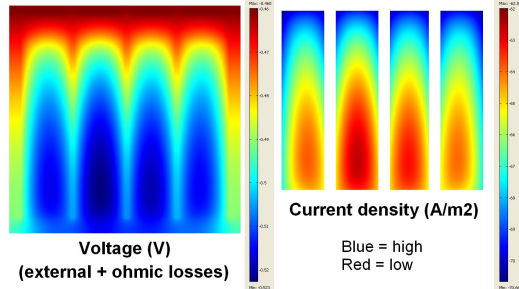
Figure 4: Voltage loss (due to substrate surface ohmic losses) and current density distribution in a 6 cm x 6 cm DSC. Main current collector is located on top of the picture.

Substrate sheet resistance Ω/sq.	η ($R_s = 0$ Ω/m) %	η ($R_s = 30$ Ω/m) %	η ($R_s = 50$ Ω/m) %	η_{loss} ($R_s = 0$ Ω/m) %	η_{loss} ($R_s = 30$ Ω/m) %	η_{loss} ($R_s = 50$ Ω/m) %
0/0	3.32	n/a	n/a	0.00	n/a	n/a
0/15	3.24	3.11	3.02	0.08	0.21	0.30
0/60	2.96	2.83	2.75	0.37	0.49	0.57
15/15	3.14	2.89	2.74	0.18	0.43	0.58
60/60	2.60	2.38	2.25	0.72	0.94	1.07

Table 1: Cell efficiencies (η) and efficiency losses (η_{loss}) calculated with different substrate sheet and current collector stripe resistance (R_s) combinations. StS sheet resistance can be approximated as zero.
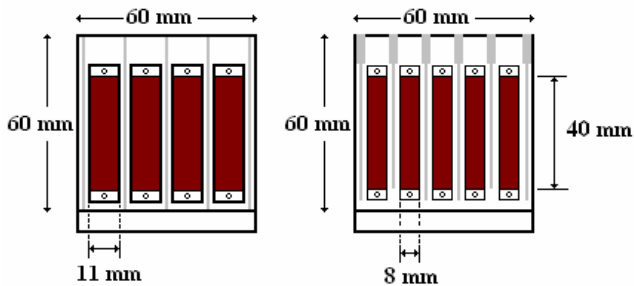
Figure 5: TiO$_2$ layer (red) and current collector (light grey) geometries for the FTO glass/ITO-PEN CE (left) and the ITO-PET CE (right) cell.
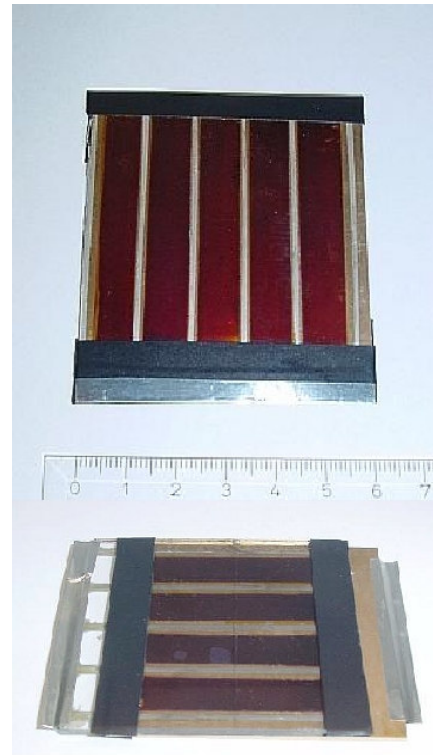
Figure 6: Photograph of the large StS-PE DSCs with ITO-PET (upper) and FTO glass (lower) CE.

3.2 Large Cell Performance

Table 2 lists the *IV*-characteristics of the best large StS-PE DSCs vs. corresponding values for a small, 0.32 cm^2 active area cell. The values obtained with our small StS-PE cells are amongst the highest reported in the literature [9, 10] and, as it can be seen from Table 2, large cell performance is not far behind. Poorer efficiency of the ITO-PEN CE cell is probably due to partial short-circuiting of the measured specimen – only a very small number of ITO-PEN CE cells were prepared – since ITO-PEN sheet resistance should be as low as that of FTO glass.

Active area cm^2	CE substr.	CE catalyst	I_{sc} mA/cm^2	V_{oc} V	FF %	η %
14.6	FTO glass	Thermal Pt	8.9	0.64	59	3.4
15.9	ITO-PET	Sputtered Pt	8.4	0.58	51	2.5
14.6	ITO-PEN	Sputtered Pt	6.6	0.61	44	1.7
0.32	ITO-PET	Sputtered Pt	10.9	0.64	49	3.4

Table 2: *IV*-parameters of the best 6 cm x 6 cm DSC "mini-modules" vs. a small DSC prepared with the same methods and materials (last row), obtained with 100 mW/cm^2 AM1.5G equivalent irradiation.

In general, the relatively low fill factors of all cells in Table 2 indicate that large cell size is not necessarily a hindrance for high cell efficiency. Instead, series resistance, i. e. the total ohmic resistance of the cell, originating from the bulk resistances of the cell materials, substrate sheet resistances and the charge transfer resistance on the CE must be lowered. This could be done for example by developing new, more conductive and catalytically active CE materials and improving the ionic conductivity in the electrolyte. Carbon-based nanomaterials such as carbon nanotubes (CNT), nanobuds (CNB) [11], and graphene sheets are potential candidates for this. A salient part of our current and near future research will concentrate on employing them in the DSC structures – for instance, graphene sheets on the CE could replace both the Pt catalyst and the conductive ITO/FTO coating.

As for cell preparation, same methods and materials that have been used for the small cells were directly upscaleable for large cells. TiO_2 layer deposition and electrolyte filling did not cause any problems though recent findings by our group indicate that the electrolyte filling direction might cause (and/or enhance) uneven current generation in a large DSC [12]. In a segmented cell (i. e. an elongated DSC where the substrates' conductive surface has been divided into parts by laser-scribing to enable spatial voltage and current measurements along the cell length) it was noticed that the open circuit voltage was higher and the short circuit current lower in those segments which were closer to the electrolyte filling hole. Since TBP is known to increase the open circuit voltage and decrease the short circuit current this indicates it might adsorb nonuniformly on the TiO_2 layer. If this is the case, new electrolyte filling techniques, e. g. spraying or printing, or replacements for TBP are needed for large DSCs.

Protection of the CE current collector stripes against the electrolyte is another remaining challenge in a large DSC. Inkjet-printing would be an ideal method for this too, the only problem being the high curing temperatures of inks suitable for this purpose. We have made preliminary tests with ITO nanoparticle ink (Ulvac) and PVP-PMF/PGMEA dielectric ink (VTT). Since the sintering temperature of the ITO ink is 230 ^{o}C and the crosslinking temperature of the dielectric ink 200 ^{o}C, vs. the maximum temperature the plastic substrates can take, 150 – 160 ^{o}C, results were not satisfactory. In soaking tests, where protective ink coated silver stripes on plastic were immersed in the electrolyte, corrosion of the silver did slow down but could not be completely stopped. This was due to porosity of the protective ink layers, caused by too low curing temperature.

4 CONCLUSIONS

We have demonstrated a large, 6 cm x 6 cm (ca. 15 cm^2 active area) DSC "mini-module" with similar efficiency than a corresponding small, 1.6 cm x 2 cm (0.32 cm^2 active area) laboratory-sized test cell. In the large cell, stainless steel works as the PE substrate, enabling drastic enlargening of the TiO_2 film size without ohmic losses, whereas the losses caused by the CE substrate sheet resistance were effectively reduced with additional current collector structures on the CE. Inkjet-printing of silver nanoparticle ink proved to be a good method for current collector deposition.

The best efficiencies obtained with our large StS-PE DSCs are 3.4 % with an FTO glass CE and 2.5 % with ITO-PET CE (cf. 3.4 % with a small, StS-PE and ITO-PET CE cell). There is still room for improvement but considering that the world record efficiencies for small DSCs prepared with the same materials and methods are around 4 % too, still, our results are very promising. Due to the inexpensive materials employed, and as the DSC lends itself for roll to roll production, the economic conditions for the structure described are very positive. The goal for the next step in our research is to achieve 5 % efficiency for a 1 by 1 foot nanosolar array.

6 REFERENCES

[1] B. O'Regan, M. Grätzel, Nature, 353, 737, 1991.
[2] http://www.dyesol.com/ , accessed January 13, 2009.
[3] K. Miettunen, J. Halme, M. Toivola, P. Lund, J. Phys. Chem. C, 112, 4011, 2008.
[4] M. Toivola, F. Ahlskog, P. Lund, Sol. Energy Mater. Sol. Cells, 90, 2881, 2006.
[5] M. Toivola, L. Peltokorpi, J. Halme, P. Lund, Sol. Energy Mater. Sol. Cells, 91, 1733, 2007.
[6] N. Papageorgiou, W. Maier, M. Grätzel, J. Electrochem. Soc., 144, 876, 1997.
[7] T. Peltola, special assignment, Helsinki University of Technology, 2008.
[8] E. Luque, S. Hegedus, Handbook of Photovoltaic Science and Engineering, Wiley, Chichester, 2003.
[9] M. Kang, N.-G. Park, K. Ryu, S. Chang, K.-J. Kim, Sol. Energy Mater. Sol. Cells, 90, 574, 2006.
[10] Y. Jun, J. Kim, M. Kang, Sol. Energy Mater. Sol. Cells, 91, 779, 2007.
[11] A. Nasibulin, P. Pikhitsa, H. Jiang, D. Brown, A. Krasheninnikov, A. Anisimov, P. Queipo, A. Moisala, D. Gonzalez, G. Lientschnig, A. Hassanien, S. Shandakov, G. Lolli, D. Resasco, M. Choi, D. Tománek, E. Kauppinen, Nature Nanotech. 2, 156, 2006.
[12] K. Miettunen, J. Halme, P. Lund, Electrochem. Comm., 11, 25, 2008.